IEEE Access
Multidisciplinary | Rapid Review | Open Access Journal

Received 13 April 2023, accepted 19 May 2023, date of publication 25 May 2023, date of current version 21 June 2023.

*Digital Object Identifier 10.1109/ACCESS.2023.3280053*

RESEARCH ARTICLE

# Gabor Contrast Patterns: A Novel Framework to Extract Features From Texture Images

**ABDUL WAHAB MUZAFFAR[1], (Member, IEEE), FARHAN RIAZ[2], TARIK ABUAIN[1], WALEED ABDEL KARIM ABU-AIN[3], FARHAN HUSSAIN[4], MUHAMMAD UMAR FAROOQ[4], AND MUHAMMAD AJMAL AZAD[5]**

[1]College of Computing and Informatics, Saudi Electronic University, Riyadh 11673, Saudi Arabia
[2]School of Computer Science, University of Lincoln, LN6 7TS Lincoln, U.K.
[3]Applied College, Taibah University, Al Madinah Al Munawwarah 42353, Saudi Arabia
[4]Department of Computer and Software Engineering, National University of Sciences and Technology, Islamabad 46000, Pakistan
[5]Department of Computer Science and Digital Technologies, Birmingham City University, B5 5JU Birmingham, U.K.

Corresponding author: Abdul Wahab Muzaffar (a.muzaffar@seu.edu.sa)

**ABSTRACT** In this paper, a novel rotation and scale invariant approach for texture classification based on Gabor filters has been proposed. These filters are designed to capture the visual content of the images based on their impulse responses which are sensitive to rotation and scaling in the images. The filter responses are rearranged according to the filter exhibiting the response having largest amplitude, followed by the calculation of patterns after binarizing the responses based on a particular threshold. This threshold is obtained as the average energy of Gabor filter responses at a particular pixel. The binary patterns are converted to decimal numbers, the histograms of which are used as texture features. The proposed features are used to classify the images from two famous texture datasets: Brodatz, CUReT and UMD texture albums. Experiments show that the proposed feature extraction method performs really well when compared with several other state-of-the-art methods considered in this paper and is more robust to noise.

**INDEX TERMS** Texture classification, Gabor filters, pattern recognition.

## I. INTRODUCTION

Texture can be defined as visual patterns appearing due to changes in contrast in the images. Quantifying visual textures is an active area of research and has been done for a wide range of applications related to remote sensing [1], [2], object recognition [3], [4], [5], image matching [6], [7] and texture classification [8] just to name a few. A major challenge in extracting texture features is to ensure their robustness under varying imaging conditions such as changes in lighting, scaling and angles of viewing. The pioneering work on texture feature extraction dates back to 1976 when gray level co-occurrence matrices were used for feature extraction from the images [9]. Phenomenal progress has since been made in the area leading to a wide range of methods, that can be divided into two main categories: model based methods and feature based methods [10]. The methods which are based on the former category use traceable models for the texture patterns where the texture analysis is based mainly on a parameter estimation task. The latter analyzes the texture as an informative description.

The use of model based methods is usually appropriate in situations where the textures are periodic or at least semi-periodic [11]. Additionally, an effective description of the texture content requires a detailed study of the underlying statistical models of the textures enforcing the need of a learning stage preceding the feature extraction stage. On the other hand, most of the feature based methods are not parametric and usually no presumption on the nature of textures is typically required, diversifying their usage for a wide range of applications. Accordingly, most of the research on texture description is based on feature based methods.

Mainly there are two types of feature based methods: statistical and signal processing based methods. Many statistical methods have been proposed to date in the literature such

The associate editor coordinating the review of this manuscript and approving it for publication was Zhan-Li Sun.

as gray level co-occurrence matrices (GLCM), local binary patterns (LBP) [12] etc giving good results. More recently, several variants of LBPs have been proposed which show very good results as compared to the standard LBPs [13], [14], [15]. These descriptors are very useful given that they can be used for the identification of different microstructures in the images such as corners, blobs, flat regions etc. which form the basis for the perception of image textures. However, these methods exhibit an inherent shortcoming given that they are based on a very local analysis and thus are relatively more sensitive to noise [16]. The signal processing based methods use filters for texture feature extraction. They offer a greater diversity since they have the ability to calculate multiresolution and multidirectional features while being able to extract both micro and macro-texture features from the images. This property is consistent with the basic characteristics of the human visual system having the visual cortex consisting of cells which are band pass filters sensitive to various scales and orientations [17]. Interestingly, the specific characteristics of *LBP* and filter based methods are complementary in nature and can be used in conjunction with one another to introduce more robust texture descriptors.

### A. CONTRIBUTIONS

In this paper, the main aim is to explore texture features having the capabilities to extract micro-texture and macro-texture features while being robust to noise. The proposed method uses Gabor filters for a macro-description and subsequently *LBP*-like differential operation for a micro-description, extracting features with characteristics which are complementary in nature and more robust to noise. The main contributions of this paper are as follows:

- Gabor Contrast Patterns (GCP): The complementary strengths of different methods are combined in *GCP* which uses Gabor kernels, resulting in mitigating noise in the images owing to the convolution operation. Later, local differential patterns are obtained from the images using an analogy derived from *LBPs* based on the responses from the Gabor filterbank.
- A visual descriptor is constructed from the *GCP* maps using the binning operation. The descriptor is analyzed for its discriminative power to represent some challenging patterns which are not adequately segregated in feature spaces by other state-of-the-art methods.
- The proposed method is quantitatively evaluated on three publicly available datasets presenting different challenges to the research community. Four different metrics including accuracy, dimensionality, noise robustness and computational complexity are used for this comparison.

The rest of the paper is organized as follows: we present the related work (Section II), followed by the proposed methodology (Section III). Later, we present our experimental results (Section IV) and conclude the paper (Section V).

## II. RELATED WORK

### A. FILTER BASED METHODS

Significant work has been done in the past on the proposal of invariant novel descriptors using filter based methods. In most of these methods, it is typically possible to decompose the visual texture information with respect to scales and orientations facilitating the calculation of invariant features. The examples of such filters include, but is not limited to Gabor filters [18], [19], [20], ridgelets [21], [22], [23], steerable filters [24], [25], [26], wavelets [27] etc. Such methods can be mainly classified into three different types. The first category of methods achieves invariance by using modified filters, or by using some trivial operations on the filter responses which compromise on some information that could be potentially useful for texture categorization. Examples of such methods include even symmetric Gabor filters [28], or filters obtained as a result of summing the direction-sensitive or scale-sensitive filters [29] to achieve rotation or scale invariant features. Since such methods are obtained as a result of compromising information across scale or orientation, the capability to represent texture characteristics is limited. The second category of methods involves the use of some sort of transformation, where possible to achieve invariance. Examples include [30], [31] in which the filter responses are subjected to post processing such as using Fast Fourier transform to obtain feature invariance. Such methods obtain good features with a drawback that the feature extraction takes place in the transform domains making the features less intuitive for visualization. An interesting category of methods involves a realignment of the feature vectors in the direction of dominant energies to achieve invariance. These strategies mitigate the effects of losses of texture information unlike the other approaches as no information related to the scales and orientations in the images is lost and the features stay in their original respective space making their visualization and comprehension simpler [32], [33], [34]. Given the simplicity of these methods, these are most widely used for the extraction of rotation and scale invariant features. However after these operations, the resulting features are typically lying in higher dimensional spaces which are not useful directly for classification purposes due to the problems of curse of dimensionality. Over the past decade, the strength of these filtering based methods has been widely utilized in the methods based on convolution neural networks that are composed of various layers including the convolutional layers which make use of filtering operation as a part of feature extraction process. Researchers have resorted to the use of statistics to resolve this issue. However it is important to note that invariably in all these methods, the richness of the texture content is compromised by the final step which prevents from performing a very fine analysis of image textures (which are actually very descriptive for texture images). This aspect of the texture descriptors (microtextures) has been thoroughly explored by the methods which are based on Local Binary Patterns (*LBP*) [35] and have been explored in this paper.

### B. LBP VARIANTS

*LBPs* have proven to be very robust for different applications requiring the extraction of rich texture features from the images. The *LBPs* exhibit a very low computational cost and are robust to environmental changes and have attracted a great interest in texture analysis leading to the proposal of different variants of *LBP* [36], [37], [35]. Guo et al. [38] proposed completed *LBP* (*CLBP*) which calculate a magnitude vector from a difference vector. They combine three complementary characteristics including magnitude and direction of local differences as well as center pixels creating a 3D histogram for texture description. Discriminative capability was further improved in feature based *LBP* (*FbLBP*), which use mean and variance to represent magnitude numbers. Several attempts have been made to propose the descriptors which are rotation and scale invariant. Dominant rotated *LBP*(*DRLBP*) calculate the local dominant direction and appropriately rotate the weights to yield rotation invariance. Scale invariance in *LBPs* has been achieved in several ways. Li et al. [39] made use of Laplacian of Gaussian to select the relevant scale at which *LBP* patterns are calculated for every pixel, thus employing a scale adaptive *LBP* radius. In scale selective *LBP*(*SSLBP*), histograms of pre-learned dominant *LBPs* are constructed and use maximum frequency among different scales as image features. Some variants of *LBP* are designed to handle noise more efficiently as *LBP* based descriptors are more sensitive to noise. In this context, Ren et al. [16] proposed noise resistant LBP (*NRLBP*) which perform error correction in the patterns, and they also proposed an extended version of these patterns *ENRLBP*. Some patch based techniques were proposed [40], [41], leading to local contrast patterns (*LCP*) using directed and undirected difference masks. Liu et al. [42] proposed binary rotation invariant and noise tolerant method (*BRINT*) method, which take the average value of the pixels in a neighborhood and calculate its binary patterns, making the resulting patterns more resistant to noise. Some variants of the *LBP* are devised to deal with color images such as color local patterns [43] multichannel decoder-based *LBP* [43] where a color pixel is treated as a vector having m-components and form a hyperplane and cube diagonal *LBP* [44], [45]. It is clear that all these methods have their own strengths and weaknesses and their characteristics are complementary to one another. In this paper, the complementary strengths of filter based methods and LBP variant are combined together to propose Gabor Contrast Patterns, which have the capability to extract texture features which are robust to noise. The methodology is discussed and evaluated for accuracy, dimensionality and noise robustness in the subsequent sections.

## III. PROPOSED METHOD

### A. GABOR FILTERS

The first step involved in feature extraction of images is Gabor filtering. Over the past decades, the Gabor filters have been widely used for applications related with texture classification. Their use is mainly motivated by the fact that the 2D Gabor filters are very similar to the visual cortex of mammals [17]. Another important consideration is that Gabor filters have the ability to achieve optimal localization in both spatial and frequency domain [46]. A Gabor filter consists of a sinusoidal plane wave with a particular frequency and orientation, modulated by a Gaussian envelope. The Gabor filtering of an image is represented by the convolution of the images with a bank of Gabor filters

$$\begin{aligned} G_{\theta,\sigma}(x,y) &= I(x,y) * \psi_{\theta,\sigma}(x,y) \\ &= \int_{k=-\infty}^{+\infty}\int_{l=-\infty}^{+\infty} I(x,y)\psi_{\theta,\sigma}(x-k,y-l) \end{aligned} \quad (1)$$

where $I(\bullet)$ denotes the input images, $\psi_{\theta,\sigma}(\bullet)$ represents the Gabor filter with an orientation $\theta$ and scale $\sigma$ and $*$ is the convolution operator. A Gabor filter can be mathematically defined as follows:

$$\psi(x,y) = \frac{f^2}{\pi\gamma\eta} e^{-\left(\frac{f^2}{\gamma^2}x'^2+\frac{f^2}{\eta^2}y'^2\right)} e^{j2\pi f x'} \quad (2)$$

$$x' = x\cos\theta + y\sin\theta$$

$$y' = -x\sin\theta + y\cos\theta \quad (3)$$

where $f$ is the central frequency of the filter, $\theta$ is the rotation angle of the major axis of the Gaussian function, $\gamma$ is the sharpness along the major axis and $\eta$ is the sharpness along the minor axis. In the given form, $\lambda = \frac{\eta}{\gamma}$ is the aspect ration of the Gaussian function. The 2D Gabor filter function in the frequency domain is

$$\Psi(u,v) = e^{\frac{-\pi^2}{f^2}\left(\gamma^2(u'-f)^2+\eta^2 v'^2\right)} \quad (4)$$

$$u' = u\cos\theta + v\sin\theta$$

$$v' = -u\sin\theta + vcos\theta \quad (5)$$

which is a bandpass filter in the frequency domain. A bank of Gabor filters is obtained by changing the parameters of a Gabor wavelet and obtaining the relevant filter banks. If $S$ is the total number of scales and $K$ is the total number of orientations at which the Gabor filters are calculated, a feature vector of size $S \times K$ for every pixel in a Gabor filtered image is obtained. The response $R_i(f_m, \theta_n)$ at $i^{th}$ pixel can be represented by the equation as in (7), shown at the bottom of the next page, where $m = 0, 1, \cdots, S-1$ is the index used for scales and $n = 0, 1, \cdots, K-1$ is the index used for orientation and $r_i(x_i, y_i, f_m, \theta_n)$ is the response of the filter bank at $i^{th}$ pixel with center frequency $f_m$ and orientation $\theta_n$. Typically, a filter bank is constructed by selecting a frequency $f_{max}$, and creating multiple filters by varying the center frequencies of the filter banks according to a certain criteria, mainly represented as

$$f_m = k^{-l} f_{max}, m = \{0, \cdots, l-1\} \quad (6)$$

where $f_m$ is the $m^{th}$ frequency, $f_0 = f_{max}$ is the highest desired frequency, and $k$ is the frequency scaling factor ($k > 1$, $k \in \mathbf{R}$).

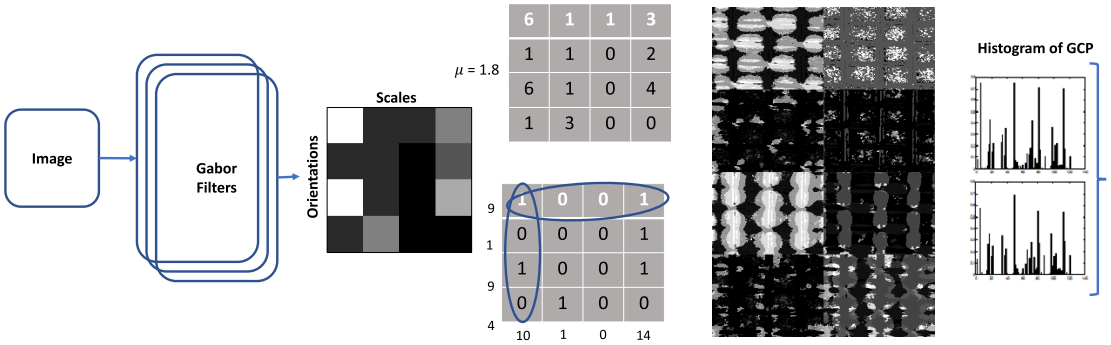


**FIGURE 1.** Visual illustration of the procedure adopted in the proposed method for generating the feature maps of Gabor Contrast Patterns. 8 feature maps are obtained in the figure, one corresponding to each scale and orientation (4 scales and 4 orientations).

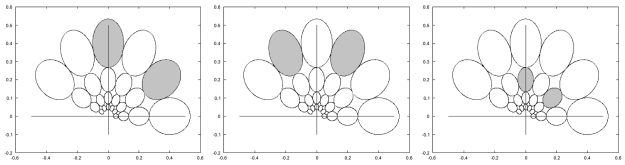

(a) Original image (b) Rotated image (c) Scaled image

**FIGURE 2.** Effect of rotation and scaling of image on Gabor responses: transfer of energy to other filter banks, dilated and rotated by the same amount as that of the image.

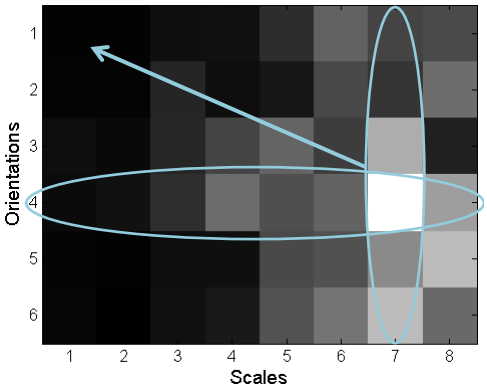


**FIGURE 3.** Applying circular rotation to align the filter response matrix by the highest energy response at the top left cell in the matrix. The Gabor filter in this figure employs 6 orientations and 8 scales.

### B. GABOR CONTRAST PATTERNS

The matrix, $R_i(f_m, \theta_n)$ obtained at the $i^{th}$ pixel has a specific characteristic: when rotation or scaling of an image takes place, these transformations will be interpreted as shift in $R_i(f_m, \theta_n)$ since the filters which are appropriately rotated and scaled will capture these transformation (Fig. 2). $R'_i(f_m, \theta_n)$ is constructed such that

$$R'_i(f_m, \theta_n) = P_r R_i(f_m, \theta_n) P_c \tag{8}$$

where $P_r$ and $P_c$ represent permutation matrices with respect to rows and columns respectively. These matrices are calculated such that the $r'_i(x_i, y_i, f_0, \theta_0)$ has the maximum value, a strategy that is similar to the one used in [34] for extraction of rotation and scale invariant Gabor responses (Fig. 3). Later, the filter responses are quantized and encoded into specific patterns which can later be used for classification. We will call the resulting features as Gabor contrast patterns (*GCP*). The basis of formulating these patterns lies on the deviation of the filter responses at specific orientations and scales from the mean of absolute values

**Algorithm 1** Gabor Contrast Patterns

**procedure** Texture feature extraction
**Input:** Images for computation of GCP
  **for** each image **do**
    Convert image to gray scale
    Perform filtering: $R(f, \theta) \leftarrow I(x, y) * \psi_{\theta,f}(x, y)$
    **for** each $i^{th}$ pixel **do**
      $R'_i(f_m, \theta_n) \leftarrow R_i(f_m, \theta_n) - E\{|R_i(f, \theta)|\}$
      Binarize $R'_i(f_m, \theta_n)$ using a sign function $s(x)$
    **end for**
    Calculate $SC_i(f_m)$ and $RC_i(\theta_n)$
  **end for**
  generate histogram of *SC* and *RC* for full image
  Concatenate *SC* and *RC* histograms
**end procedure**

$$R_i(f_m, \theta_n) = \begin{bmatrix} r_i(x_i, y_i; f_0, \theta_0) & r_i(x_i, y_i, f_1, \theta_0) & \dots & r_i(x_i, y_i, f_{S-1}, \theta_0) \\ r_i(x_i, y_i; f_0, \theta_1) & r_i(x_i, y_i, f_1, \theta_1) & \dots & r_i(x_i, y_i, f_{S-1}, \theta_1) \\ \vdots & \vdots & \ddots & \vdots \\ r_i(x_i, y_i; f_0, \theta_{K-1}) & r_i(x_i, y_i, f_1, \theta_{K-1}) & \dots & r_i(x_i, y_i, f_{S-1}, \theta_{K-1}) \end{bmatrix} \tag{7}$$

of filter responses at each pixel (Fig. 1). Let us define $dR'_i(f_m, \theta_n) = R'_i(f_m, \theta_n) - th_i$, where $th_i$ is given as follows:

$$th_i = \frac{1}{S \times K} \sum_{m=0}^{S-1} \sum_{n=0}^{K-1} |R'_i(f_m, \theta_n)| \tag{9}$$

The deviation of a pixel response from the average energy of a pixel is quantized using $s(dR_i(f_m, \theta_n))$, where $s(\bullet)$ is a sign function such that

$$s(x) = \begin{cases} 1 & x \geq th_i \\ 0 & x < th_i. \end{cases} \tag{10}$$

Later, the codes based on this binary matrix are constructed using which the feature vector is calculated.

#### 1) SCALE CONTRAST

At a particular scale, the contrast codes for the directional information is in the $m^{th}$ column of $dR'_i$. The binary code in this column can be used to construct a decimal code as follows (Fig. 1):

$$SC_i(f_m) = \sum_{k=0}^{K-1} s(dR'_i(f_m, \theta_n))2^k \tag{11}$$

The $SC_i(f_m)$ indicates a contrast pattern at $m^{th}$ Gabor filter scale, calculated for the $i^{th}$ pixel. Given that Gabor filtering has been performed at $S$ different scales, as many number of scale contrast patterns can be constructed.

#### 2) ROTATION CONTRAST

At a particular orientation, the contrast codes for the scale information corresponds to the $k^{th}$ row of $dR'_i$. The binary code for this row of $dR'_i$ can be used to construct a decimal code as follows (Fig. 1):

$$RC_i(\theta_n) = \sum_{k=0}^{S-1} s(dR'_i(f_m, \theta_n))2^k \tag{12}$$

The $RC_i(\theta_n)$ indicates a contrast pattern at $n^{th}$ Gabor filter orientation, calculated for the $i^{th}$ pixel. A total of $K$ rotation contrast patterns can be constructed for a particular pixel.

### C. HISTOGRAM OF CONTRAST PATTERNS

After the extraction of the contrast patterns, their histograms are constructed. For Gabor filters with $S$ scales and $K$ orientations, a total of $S \times K$ histograms are constructed.

$$GCP = \begin{bmatrix} \mathcal{F}_{f_1}(SC) & \dots & & \\ \mathcal{F}_{f_m}(SC) & \mathcal{F}_{\theta_1}(RC) & \dots & \mathcal{F}_{\theta_n}(RC) \end{bmatrix} \tag{13}$$

where $\mathcal{F}(\bullet)$ is the frequency of occurrence of a particular pattern. The histograms obtained from the scale and rotation contrasts are concatenated to form a feature vector. After obtaining the representation features for an image, standard machine learning methods can be used for classification of the images A visual illustration of the proposed method is shown in Fig. 1.

### D. ANALYSIS OF GCP

The proposed texture feature set exhibits unique characteristics, which are not shared by the existing feature extraction techniques. The Gabor filters are obtained by the multiplication of a Gaussian filter with sinusoidal function. Effectively, this means that the use of Gaussian function in formulating the impulsive responses smoothes the images inherently performing noise removal from the images. When the contrast patterns are calculated at each pixel, this noise removal plays a key role where only the real texture content which is visualized by variations in the gray level values in the images is remaining and the noisy variations in the images are catered for by the Gaussian function in the filtering step. Thus, a texture descriptor which has the ability to capture fine texture in the images, while not being very sensitive to noise is obtained. This is a unique contribution given that the existing methods employing Gabor filters are usually based on statistics which do not capture local texture content. Some existing techniques are based on the calculation of local binary patterns on the Gabor filtered images but these techniques calculate the texture features individually from each lattice plane in the Gabor filters and do not fuse the decomposed texture content at various scales and orientations. Most of the local visual descriptors typically cannot discriminate between some specific patterns, although they are visually different (Some specific examples have been considered in Fig. 4). It is visually evident that the first two rows, which represent the local binary patterns (*LBP*) and local ternary patterns (*LTP*) do not yield discriminative features whereas the proposed features are robust and have the ability to differentiate between the images shown in the first row. From these representative patterns, it is clear that the discriminative power of the proposed descriptors is increased as the feature space looks visually different for the patterns which are considered in the image. Although the figure demonstrates the discriminative ability of the proposed features, the representation for noisy texture will be quantitatively presented in the results section.

## IV. EXPERIMENTAL RESULTS AND ANALYSIS

To validate the effectiveness of *GCP*, several experiments were carried out in this paper, which are as follows:

### A. EXPERIMENTAL SETUP

For our experiments, three different datasets have been used: Brodatz, CuRET and UMD having their own respective challenges (Table 2). Brodatz is a challenging texture album having a collection of around 111 textures. Generally, the textures look very different with some of them being particularly difficult given that similar textures acquired at different scales have to be classified into different categories. This is particularly challenging for the descriptors which are scale invariant as they will lead to wrong classifications for such cases (Fig. 6). In the CuRET dataset, the image have been acquired under varying lighting conditions from arbitrary viewpoints, emulating acquisition of the same images under

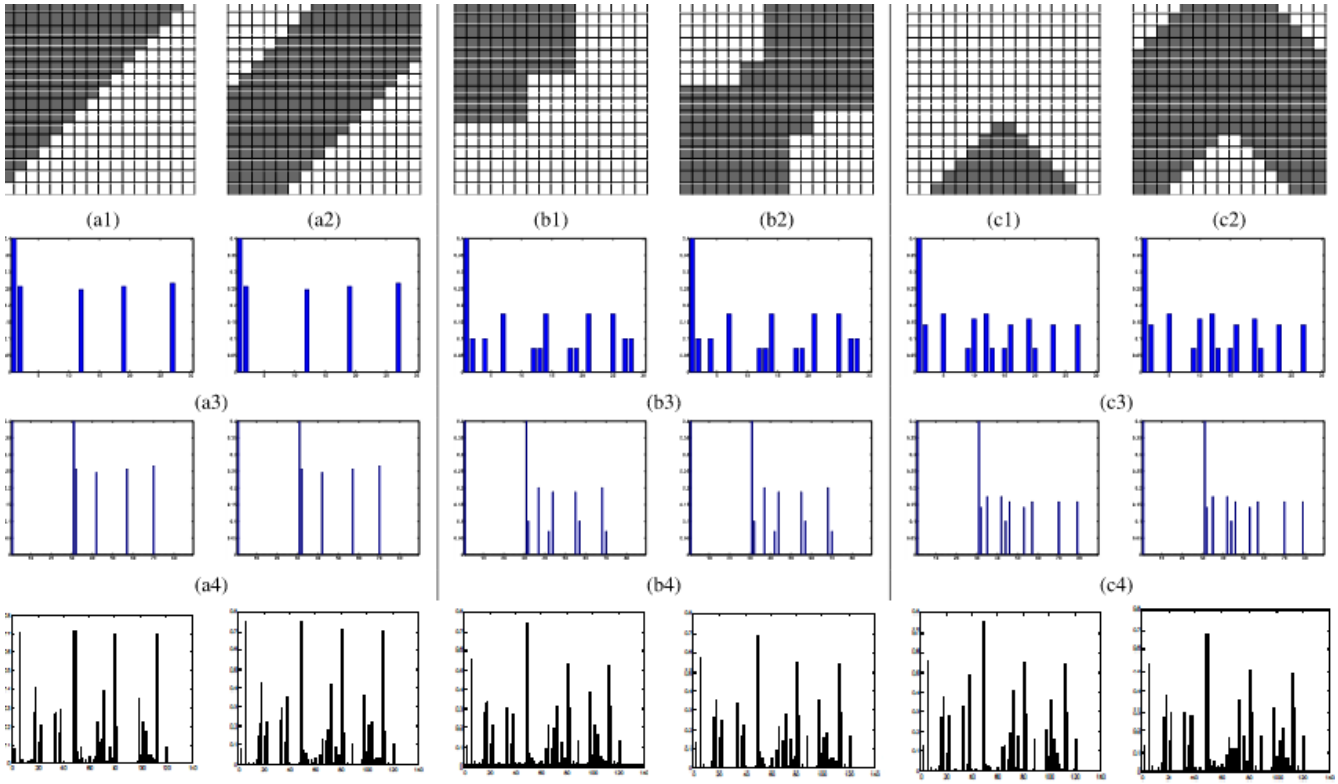


**FIGURE 4.** The figure identifies the problems exhibited by the standard local descriptors. The first row indicates the original images, second row shows the histograms of local binary patterns (LBP), third row shows the histogram of local ternary patterns and the fourth row indicates the features obtained using the proposed Gabor contrast patterns (GCP). The visualization of features shows that GCP exhibits the capability to discriminate between different textures which yield similar features in comparison to other local descriptors (partially adapted from [14]).

**TABLE 1.** Summary of feature extraction methods compared with the proposed descriptor.

| Methods | Acronym | Year | Ref | Publication |
|---|---|---|---|---|
| Local Binary Patterns | $LBP$ | 1996 | [35] | Pattern Recognition |
| Rotation invariant Uniform Local Binary Patterns | $LBP_{riu2}$ | 2002 | [35] | IEEE trans Pattern Analysis and Machine Intelligence |
| Rotation invariant Local Binary Patterns | $LBP_{ri}$ | 2002 | [35] | IEEE trans Pattern Analysis and Machine Intelligence |
| Improved Local Binary Patterns | $ILBP$ | 2016 | [47] | IEEE ICASSP |
| Completed Local Binary Patterns | $CLBP$ | 2004 | [38] | IEEE trans on Image Processing |
| Median Binary Patterns | $MBP$ | 2007 | [48] | Springer ICIAR |
| Rotation Invariant Median Binary Patterns | $MBP_{riu2}$ | 2008 | [48] | Conference on Pattern Analysis and Recognition |
| Robust Local Binary Patterns | $RLBP$ | 2013 | [49] | British Machine Vision Conference |
| Extended Local Binary Patterns | $EXLBP$ | 2008 | [50] | Information Sciences |
| Noise Tolerant Local Binary Patterns | $NTLBP$ | 2012 | [51] | Pattern Recognition Letters |
| Multi-Dimensional Local Binary Patterns | $MDLBP_{riu2}$ | 2012 | [52] | International Conference on Pattern Recognition |
| Dominant Local Binary Patterns | $DLBP$ | 2009 | [53] | IEEE trans on Image Processing |
| Binary Rotation Invariant Noise Tolerant | $BRINT$ | 2014 | [42] | IEEE trans on Image Processing |
| Local Binary Pattern Difference | $LBPD$ | 2014 | [54] | IEEE trans on Image Processing |
| Scale Selective Local Binary Patterns | $SSLBP$ | 2015 | [55] | IEEE trans on Image Processing |
| Adaptive Median Binary Patterns | $AMBP$ | 2015 | [56] | Pattern Recognition |
| Medium Robust Extended LBP | $MRELBP$ | 2016 | [57] | IEEE trans on Image Processing |
| Robust Adaptive Median Binary Patterns | $RAMBP$ | 2019 | [58] | IEEE trans on Image Processing |
| Local Grouped Ordered Non-Local Binary Patterns | $LGONBP$ | 2021 | [59] | IEEE trans on Circuits and Systems for Video Technology |

different rotation and scale variations. Therefore this dataset is very useful to assess the rotation and scale invariant properties of the descriptors (Fig. 7). A similar set of characteristics are exhibited by the UMD dataset in which the validation of rotation and scale invariant characteristics can be done (Fig. 8).

For feature extraction Gabor filters are used, having two important parameters as discussed earlier: number of scales and orientations. These parameters impact the method in two distinct ways: 1). An increase in the number of scales and orientation increases the number of dimensions, and 2). Increase in computational complexity as adding more scales

**TABLE 2.** Description of datasets used for the experiments.

| Name | Description | Image Size | Classes | Samples |
|---|---|---|---|---|
| Brodatz | Images are given in different background intensities. The size of each image in the Brodatz album is 512×512. Each image in the album is divided into 16 non-overlapping regions, each of size 128x128 giving a total of 1776 images. | 128 × 128 | 111 | 90 |
| CuRET | This database is designed to have a wide intra-class variation. The images are acquired under different lighting conditions from arbitrary viewpoints inserting a strong rotation and scale variations among images of the same type. | 640 × 480 | 61 | 92 |
| UMD | This dataset is composed of a set of images belonging to the same texture, having acquired from different viewpoints. Therefore, the images with same texture exhibit a significant variation in scale and rotation changes. The illumination changes in the images are marginal. | 1280 × 960 | 25 | 40 |

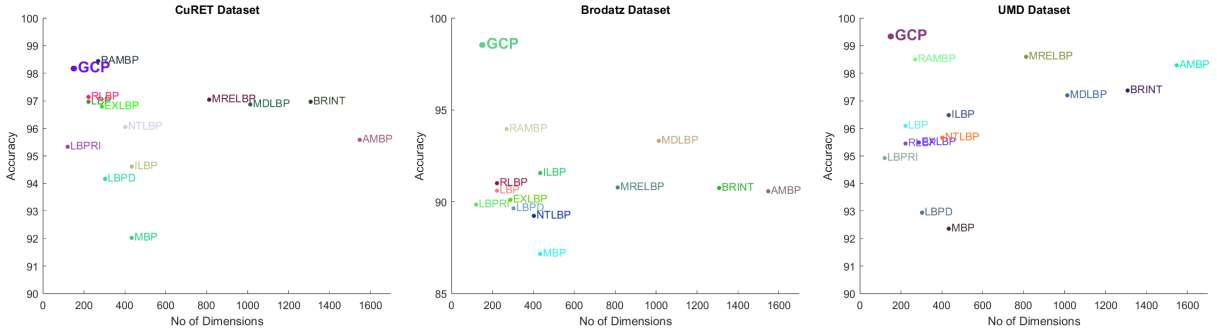


**FIGURE 5.** Visual comparison of the methods as a tradeoff between their classification accuracies and feature dimensions.

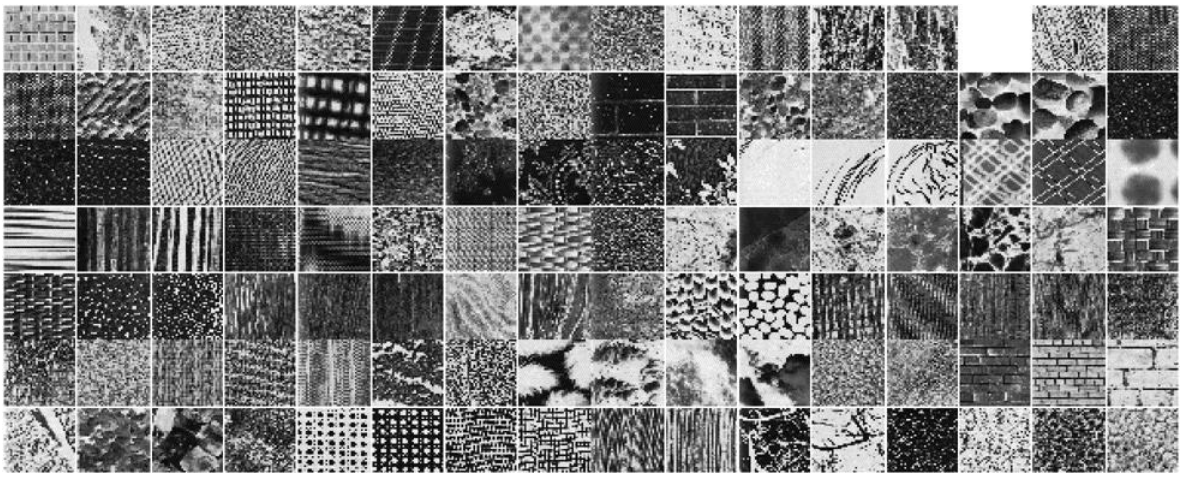

**FIGURE 6.** Sample images from 111 texture classes in the Brodatz dataset.

and orientations increases the number of filter banks requiring more convolutional operations to conclude the feature extraction process. For the purpose of our experiments, four scales and four orientations have been used. Although this number can be increased to increase the richness of the feature extraction process, the parameters are chosen as a result of grid search where an increase in these parameters gives an almost similar or marginal improvement on classification results. For classification, one nearest neighbor method has been used. The performance of the proposed method has been compared with several other methods which are highlighted in Table 1. The proposed method has been evaluated on three different parameters including classification accuracy, the dimensionality and algorithm running time. The experiments have been carried out on a 7 Duo 3.5 GHz processor with 32 GB RAM in Matlab 2017b.

### B. OVERALL RESULTS

Generally, the results obtained for CuRET and UMD are better. Although the main objective of these datasets is to perform testing of invariance by incorporating visualization of images belonging to a similar class, potentially leading to somewhat similar samples appearing in the training and testing sets, and hence the better accuracies for both of these

**TABLE 3.** Classification results obtained using different texture feature extraction methods.

| Methods<br># classes | CuRET<br>(61) | Brodatz<br>(111) | UMD<br>(25) |
|---|---|---|---|
| $LBP$ | 92.77 | 88.67 | 96.80 |
| $LBP_{riu2}$ | 97.03 | 90.70 | 96.15 |
| $LBP_{ri}$ | 95.38 | 89.93 | 94.99 |
| $ILBP_{rui2}$ | 94.66 | 91.66 | 96.54 |
| $CLBP$ | 97.33 | 92.34 | 98.62 |
| $MBP_{riu2}$ | 92.09 | 87.25 | 92.41 |
| $MBP$ | 91.24 | 89.27 | 95.64 |
| $RLBP_{riu2}$ | 97.20 | 91.09 | 95.50 |
| $EXLBP$ | 96.85 | 90.19 | 95.55 |
| $NTLBP$ | 96.11 | 89.31 | 95.72 |
| $MDLBP_{riu2}$ | 96.92 | 93.40 | 97.26 |
| $DLBP$ | 94.38 | 88.73 | 93.58 |
| $BRINT$ | 97.02 | 90.83 | 97.44 |
| $LBPD$ | 94.23 | 89.74 | 92.99 |
| $SSLBP$ | 98.79 | 89.94 | 98.40 |
| $AMBP$ | 95.64 | 90.67 | 98.34 |
| $MRELBP$ | 97.10 | 90.86 | 98.66 |
| $RAMBP$ | **98.50** | 94.05 | 98.57 |
| $LGONBP$ | 97.43 | 92.43 | 97.70 |
| $GCP$ | 98.25 | **97.65** | **99.41** |

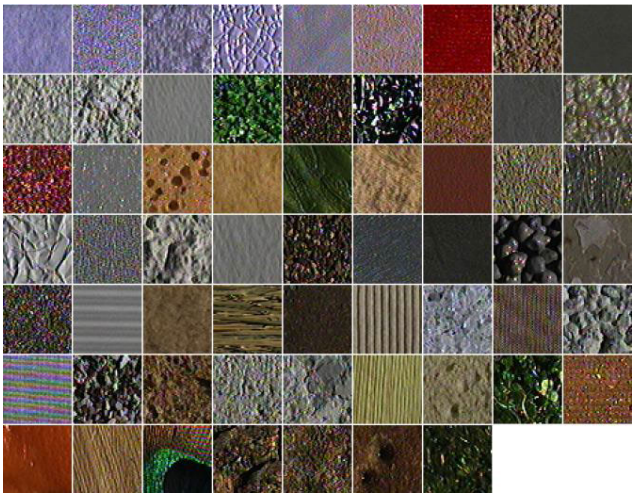

**FIGURE 7.** Samples images from 92 texture classes in Columbia-Utrecht dataset.

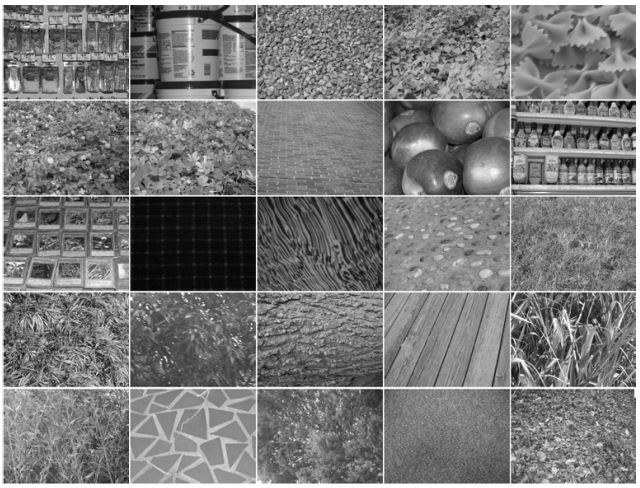

**FIGURE 8.** Sample image from 25 texture classes in UMD dataset.

**TABLE 4.** Comparison between different methods in terms of computational complexity.

| Methods | Dimensionality | Time (ms) |
|---|---|---|
| $LBP_{riu2}$ | 210 | 87.2 |
| $LBP_{ri}$ | 108 | **47.5** |
| $ILBP_{rui2}$ | 420 | 90.8 |
| $CLBP$ | 3552 | 127.9 |
| $MBP_{riu2}$ | 420 | 215.6 |
| $RLBP_{riu2}$ | 210 | 488.6 |
| $EXLBP$ | 273 | 91.3 |
| $NTLBP$ | 388 | 332.3 |
| $MDLBP_{riu2}$ | 1000 | 26.3 |
| $DLBP$ | 14150 | 565.3 |
| $BRINT$ | 1296 | 248.8 |
| $LBPD$ | 289 | 54.2 |
| $SSLBP$ | 2400 | 180.0 |
| $AMBP$ | 1536 | 92.5 |
| $MRELBP$ | 800 | 416.6 |
| $RAMBP$ | 256 | 480.3 |
| $LGONBP$ | 1404 | 164 |
| $GCP$ | **128** | 771.4 |

**TABLE 5.** Classification results obtained on noisy and noise-free CuRET dataset.

| Methods | Noise free | SNR (dB) | | | |
|---|---|---|---|---|---|
| | | 5 | 10 | 15 | 30 |
| $LBP$ | 92.77 | 58.55 | 67.93 | 72.80 | 78.98 |
| $CLBP$ | 97.33 | 69.03 | 79.51 | 84.49 | 90.17 |
| $MRELBP$ | 97.10 | 76.23 | 84.92 | 88.95 | 92.44 |
| $BRINT$ | 97.02 | 85.04 | 90.78 | 93.51 | 95.14 |
| $LGONBP$ | 95.01 | 83.58 | 89.20 | 91.55 | 93.54 |
| $GCP$ | 98.25 | 88.95 | 91.23 | 93.59 | 96.63 |

datasets (Table 3). Arguably, a similar situation is also faced by the Brodatz album for images where the granularity of the texture is very high and thus the possibilities of repetitiveness become higher, but there are some other cases which become very challenging where the texture is not fine grained. The observation is endorsed by the fact that for *SSLBP*, *RAMBP* and *GCP*, the results obtained on the Brodatz album are surpassing 98% showing that the methods making appropriate adjustments to the scale of the images show better results in contrast to their other counterparts.

Results show that the proposed method performs better for both the Brodatz and UMD dataset. It always does well on the CuRET dataset, however, the *RAMBP* shows the best classification accuracies. There are some specific interesting observations which can be deduced from the results. Generally, it is a coherent observation that for the rotationally invariant schemes which are purely based on LBPs the overall accuracies tend to decrease. Using *LBP* and *MBP* gives better results in contrast to their invariant counterparts. This happens because the concept of rotational invariance is induced in the LBPs by characterising a specific edge across all

directions into a single category and this deceases the discriminative capability of the descriptors.

Another important aspect is the computational complexity of the descriptor. It is well known that the *LBP* based descriptors are highly efficient with respect to the computation time as they are based simply on the calculation of a difference value followed by thresholding. Appropriately, it can be seen that $LBP_{ri}$ is the most efficient descriptor taking only 47.5ms to complete the computations for an images and the *GCP* is the computationally most expensive descriptor (Table 4). This performance is attributed to the convolution operation while performing Gabor filtering which requires a significant number of computational resources. It should be noted that the method is parametric and the computation time for a specific images is a function of the number of scales and orientations, which have been chosen as a result of grid search of these parameters to tradeoff accuracies, computation time and dimensionality of the descriptor.

Among that the methods which have been considered in this paper, *GCP* is the most powerful descriptor with compact energy exhibited within only 128 features, and delivering very good results on large datasets (CuRET with 2806 test images over 61 classes and Brodatz with 4995 test images over 111 classes) which is a challenging task for a descriptor. The close competitors of *GCP* include *RAMBP* which has double the number of features (in comparison to *GCP* - Fig. 5). Finally, experiments have been performed to validate the robustness of *GCP* to noise in Table 5. This has been done by generating Gaussian noise with different values of $\sigma$ and adding it to the images to prepare their noisy counterparts. As can be seen in the table, the standard *LBP* are highly sensitive to noise, with other variants of *LBP* showing relatively good results in the presence of noise. *GCP* shows the highest level of robustness to noise elucidating on the strength of the proposed descriptor in the presence of noise in the images. These results are attributed to the Gaussian filtering involved while filtering the images, which results in the mitigation of noise in the images.

## V. CONCLUSION

This paper proposes a novel visual descriptor that can be used for the classification of texture images. This descriptor is based on Gabor filters given that they offer the diversity of calculating multiresolution and multidirectional features. The nature of these filters is consistent with the human visual system where the cells in the visual cortex are sensitive to directions and scales of the visual scene. A matrix representing the filter responses to individual filters sensitive to the directions and scales is constructed. Circular shifts to this matrix are applied such that the response of the filter representing the maximum amplitude lies on the top left corner of the matrix. Later on, the average absolute energy of the pixel is subtracted from the matrix followed by its binarization. These binary codes are used to construct the decimal codes which can represent the features at a particular pixel. A histogram of these codes is generated that can be used for the classification of the images using standard machine learning methods.

The performance of the proposed descriptor has been evaluated on three widely known texture datasets in the literature: 1). Brodatz, and 2). CUReT, and 3). UMD datasets. For assessing the relative performance of the proposed approach, different methods based on the Local Binary Patterns (*LBP*) have been chosen. Our method performs favorably as compared to the other methods considered in this paper. *GCP* is also the most compact descriptor with respect to the dimensionality and thus can be considered most discriminative in the feature space. However, the computation time for *GCP* is higher due to the use of convolutional operator for an entire filterbank.

Although the proposed descriptor performs well, it requires wider validation across different datasets. Therefore, in the future, we aim to perform our experiments on more challenging datasets to validate the strength of the features produced by *GCP*.

## REFERENCES

[1] J. Yuan, D. Wang, and R. Li, "Remote sensing image segmentation by combining spectral and texture features," *IEEE Trans. Geosci. Remote Sens.*, vol. 52, no. 1, pp. 16–24, Jan. 2014.

[2] Y. Zhao, L. Zhang, P. Li, and B. Huang, "Classification of high spatial resolution imagery using improved Gaussian Markov random-field-based texture features," *IEEE Trans. Geosci. Remote Sens.*, vol. 45, no. 5, pp. 1458–1468, May 2007.

[3] X. Wu and B. Bhanu, "Gabor wavelet representation for 3-D object recognition," *IEEE Trans. Image Process.*, vol. 6, no. 1, pp. 47–64, Jan. 1997.

[4] Y. Kang, K. Kidono, T. Naito, and Y. Ninomiya, "Multiband image segmentation and object recognition using texture filter banks," in *Proc. 19th Int. Conf. Pattern Recognit.*, Dec. 2008, pp. 1–4.

[5] J. Wang and Y. Yagi, "Integrating color and shape-texture features for adaptive real-time object tracking," *IEEE Trans. Image Process.*, vol. 17, no. 2, pp. 235–240, Feb. 2008.

[6] J. Yue, Z. Li, L. Liu, and Z. Fu, "Content-based image retrieval using color and texture fused features," *Math. Comput. Model.*, vol. 54, nos. 3–4, pp. 1121–1127, Aug. 2011.

[7] Y. Rui, T. S. Huang, and S.-F. Chang, "Image retrieval: Current techniques, promising directions, and open issues," *J. Vis. Commun. Image Represent.*, vol. 10, no. 1, pp. 39–62, Mar. 1999.

[8] B. S. Manjunath and W. Y. Ma, "Texture features for browsing and retrieval of image data," *IEEE Trans. Pattern Anal. Mach. Intell.*, vol. 18, no. 8, pp. 837–842, Aug. 1996.

[9] L. S. Davis, S. A. Johns, and J. K. Aggarwal, "Texture analysis using generalized co-occurrence matrices," *IEEE Trans. Pattern Anal. Mach. Intell.*, vol. PAMI-1, no. 3, pp. 251–259, Jul. 1979.

[10] I. Kokkinos, G. Evangelopoulos, and P. Maragos, "Texture analysis and segmentation using modulation features, generative models, and weighted curve evolution," *IEEE Trans. Pattern Anal. Mach. Intell.*, vol. 31, no. 1, pp. 142–157, Jan. 2009.

[11] S. Selvan and S. Ramakrishnan, "SVD-based modeling for image texture classification using wavelet transformation," *IEEE Trans. Image Process.*, vol. 16, no. 11, pp. 2688–2696, Nov. 2007.

[12] T. Ojala, M. Pietikäinen, and D. Harwood, "A comparative study of texture measures with classification based on featured distributions," *Pattern Recognit.*, vol. 29, no. 1, pp. 51–59, Jan. 1996.

[13] K. Wang, C. Bichot, C. Zhu, and B. Li, "Pixel to patch sampling structure and local neighboring intensity relationship patterns for texture classification," *IEEE Signal Process. Lett.*, vol. 20, no. 9, pp. 853–856, Sep. 2013.

[14] A. Satpathy, X. Jiang, and H. Eng, "LBP-based edge-texture features for object recognition," *IEEE Trans. Image Process.*, vol. 23, no. 5, pp. 1953–1964, May 2014.

[15] K.-C. Fan and T.-Y. Hung, "A novel local pattern descriptor—Local vector pattern in high-order derivative space for face recognition," *IEEE Trans. Image Process.*, vol. 23, no. 7, pp. 2877–2891, Jul. 2014.

[16] J. Ren, X. Jiang, and J. Yuan, "Noise-resistant local binary pattern with an embedded error-correction mechanism," *IEEE Trans. Image Process.*, vol. 22, no. 10, pp. 4049–4060, Oct. 2013.

[17] D. J. Field, "Relations between the statistics of natural images and the response properties of cortical cells," *J. Opt. Soc. Amer. A, Opt. Image Sci.*, vol. 4, no. 12, p. 2379, 1987.

[18] V. Kyrki, J.-K. Kamarainen, and H. Kälviäinen, "Simple Gabor feature space for invariant object recognition," *Pattern Recognit. Lett.*, vol. 25, no. 3, pp. 311–318, Feb. 2004.

[19] F. Riaz, A. Hassan, R. Nisar, M. Dinis-Ribeiro, and M. T. Coimbra, "Content-adaptive region-based color texture descriptors for medical images," *IEEE J. Biomed. Health Informat.*, vol. 21, no. 1, pp. 162–171, Jan. 2017.

[20] M. M. Damaneh, F. Mohanna, and P. Jafari, "Static hand gesture recognition in sign language based on convolutional neural network with feature extraction method using ORB descriptor and Gabor filter," *Expert Syst. Appl.*, vol. 211, Jan. 2023, Art. no. 118559.

[21] P. Rayavel and C. Murukesh, "Comparative analysis of deep learning classifiers for diabetic retinopathy identification and detection," *Imag. Sci. J.*, vol. 70, no. 6, pp. 358–370, 2023.

[22] X. Qian, F. Liu, L. Jiao, X. Zhang, Y. Guo, X. Liu, and Y. Cui, "Ridgelet-nets with speckle reduction regularization for SAR image scene classification," *IEEE Trans. Geosci. Remote Sens.*, vol. 59, no. 11, pp. 9290–9306, Nov. 2021.

[23] M. M. Feraidooni and D. Gharavian, "A new approach for rotation-invariant and noise-resistant texture analysis and classification," *Mach. Vis. Appl.*, vol. 29, no. 3, pp. 455–466, Apr. 2018.

[24] S. Paul, A. Norkin, and A. C. Bovik, "On visual masking estimation for adaptive quantization using steerable filters," *Signal Process., Image Commun.*, vol. 96, Aug. 2021, Art. no. 116290.

[25] H. Naderi, L. Goli, and S. Kasaei, "Scale equivariant CNNs with scale steerable filters," in *Proc. Int. Conf. Mach. Vis. Image Process. (MVIP)*, Feb. 2020, pp. 1–5.

[26] V. Dudar and V. Semenov, "Spatial transformer steerable nets for rotation and flip invariant classification," in *Advances in Computer Science for Engineering and Education III 3*. Cham, Switzerland: Springer, 2021, pp. 363–372.

[27] A. M. Shamaileh, T. H. Rassem, L. S. Chuin, and O. N. A. Sayaydeh, "A new feature-based wavelet completed local ternary pattern (feat-WCLTP) for texture image classification," *IEEE Access*, vol. 8, pp. 28276–28288, 2020.

[28] R. Manthalkar, P. K. Biswas, and B. N. Chatterji, "Rotation invariant texture classification using even symmetric Gabor filters," *Pattern Recognit. Lett.*, vol. 24, no. 12, pp. 2061–2068, Aug. 2003.

[29] J. Han and K.-K. Ma, "Rotation-invariant and scale-invariant Gabor features for texture image retrieval," *Image Vis. Comput.*, vol. 25, no. 9, pp. 1474–1481, Sep. 2007.

[30] F. Riaz, A. Hassan, S. Rehman, and U. Qamar, "Texture classification using rotation- and scale-invariant Gabor texture features," *IEEE Signal Process. Lett.*, vol. 20, no. 6, pp. 607–610, Jun. 2013.

[31] F. Riaz, F. B. Silva, M. D. Ribeiro, and M. T. Coimbra, "Invariant Gabor texture descriptors for classification of gastroenterology images," *IEEE Trans. Biomed. Eng.*, vol. 59, no. 10, pp. 2893–2904, Oct. 2012.

[32] X. Xie, "Efficient rotation- and scale-invariant texture classification method based on Gabor wavelets," *J. Electron. Imag.*, vol. 17, no. 4, Oct. 2008, Art. no. 043026.

[33] G. M. Haley and B. S. Manjunath, "Rotation-invariant texture classification using a complete space-frequency model," *IEEE Trans. Image Process.*, vol. 8, no. 2, pp. 255–269, Feb. 1999.

[34] J.-K. Kamarainen, V. Kyrki, and H. Kalviainen, "Invariance properties of Gabor filter-based features-overview and applications," *IEEE Trans. Image Process.*, vol. 15, no. 5, pp. 1088–1099, May 2006.

[35] T. Ojala, M. Pietikainen, and T. Maenpaa, "Multiresolution gray-scale and rotation invariant texture classification with local binary patterns," *IEEE Trans. Pattern Anal. Mach. Intell.*, vol. 24, no. 7, pp. 971–987, Jul. 2002.

[36] H. Shih, H. Cheng, and J. Fu, "Image classification using synchronized rotation local ternary pattern," *IEEE Sensors J.*, vol. 20, no. 3, pp. 1656–1663, Feb. 2020.

[37] S. Brahnam, L. C. Jain, L. Nanni, and A. Lumini, *Local Binary Patterns: New Variants and Applications*, vol. 506. Cham, Switzerland: Springer, 2014.

[38] Z. Guo, L. Zhang, and D. Zhang, "A completed modeling of local binary pattern operator for texture classification," *IEEE Trans. Image Process.*, vol. 19, no. 6, pp. 1657–1663, Jun. 2010.

[39] Z. Li, G. Liu, Y. Yang, and J. You, "Scale- and rotation-invariant local binary pattern using scale-adaptive texton and subuniform-based circular shift," *IEEE Trans. Image Process.*, vol. 21, no. 4, pp. 2130–2140, Apr. 2012.

[40] S. Liao, X. Zhu, Z. Lei, L. Zhang, and S. Z. Li, "Learning multi-scale block local binary patterns for face recognition," in *Proc. Int. Conf. Biometrics*. Cham, Switzerland: Springer, 2007, pp. 828–837.

[41] T. Song, H. Li, F. Meng, Q. Wu, B. Luo, B. Zeng, and M. Gabbouj, "Noise-robust texture description using local contrast patterns via global measures," *IEEE Signal Process. Lett.*, vol. 21, no. 1, pp. 93–96, Jan. 2014.

[42] L. Liu, Y. Long, P. W. Fieguth, S. Lao, and G. Zhao, "BRINT: Binary rotation invariant and noise tolerant texture classification," *IEEE Trans. Image Process.*, vol. 23, no. 7, pp. 3071–3084, Jul. 2014.

[43] N. Richard, R. Martinez, and C. Fernandez, "Colour local pattern: A texture feature for colour images," *J. Int. Colour Assoc.*, vol. 16, pp. 56–68, Mar. 2016.

[44] C. Singh, E. Walia, and K. P. Kaur, "Color texture description with novel local binary patterns for effective image retrieval," *Pattern Recognit.*, vol. 76, pp. 50–68, Apr. 2018.

[45] R. Tekin, Ö. F. Ertuğrul, and Y. Kaya, "New local binary pattern approaches based on color channels in texture classification," *Multimedia Tools Appl.*, vol. 79, nos. 43–44, pp. 32541–32561, Nov. 2020.

[46] G. H. Granlund, "In search of a general picture processing operator," *Comput. Graph. Image Process.*, vol. 8, no. 2, pp. 155–173, Oct. 1978.

[47] H. Jin, Q. Liu, H. Lu, and X. Tong, "Face detection using improved LBP under Bayesian framework," in *Proc. 3rd Int. Conf. Image Graph. (ICIG)*, Dec. 2004, pp. 306–309.

[48] A. Hafiane, G. Seetharaman, and B. Zavidovique, "Median binary pattern for textures classification," in *Proc. Int. Conf. Image Anal. Recognit.* Cham, Switzerland: Springer, 2007, pp. 387–398.

[49] J. Chen, V. Kellokumpu, G. Zhao, and M. Pietikäinen, "RLBP: Robust local binary pattern," in *Proc. BMVC*, 2013, pp. 1–10.

[50] H. Zhou, R. Wang, and C. Wang, "A novel extended local-binary-pattern operator for texture analysis," *Inf. Sci.*, vol. 178, no. 22, pp. 4314–4325, Nov. 2008.

[51] A. Fathi and A. R. Naghsh-Nilchi, "Noise tolerant local binary pattern operator for efficient texture analysis," *Pattern Recognit. Lett.*, vol. 33, no. 9, pp. 1093–1100, Jul. 2012.

[52] G. Schaefer and N. P. Doshi, "Multi-dimensional local binary pattern descriptors for improved texture analysis," in *Proc. 21st Int. Conf. Pattern Recognit. (ICPR)*, Nov. 2012, pp. 2500–2503.

[53] S. Liao, M. W. K. Law, and A. C. S. Chung, "Dominant local binary patterns for texture classification," *IEEE Trans. Image Process.*, vol. 18, no. 5, pp. 1107–1118, May 2009.

[54] X. Hong, G. Zhao, M. Pietikäinen, and X. Chen, "Combining LBP difference and feature correlation for texture description," *IEEE Trans. Image Process.*, vol. 23, no. 6, pp. 2557–2568, Jun. 2014.

[55] Z. Guo, X. Wang, J. Zhou, and J. You, "Robust texture image representation by scale selective local binary patterns," *IEEE Trans. Image Process.*, vol. 25, no. 2, pp. 687–699, Feb. 2016.

[56] A. Hafiane, K. Palaniappan, and G. Seetharaman, "Joint adaptive median binary patterns for texture classification," *Pattern Recognit.*, vol. 48, no. 8, pp. 2609–2620, Aug. 2015.

[57] L. Liu, S. Lao, P. W. Fieguth, Y. Guo, X. Wang, and M. Pietikäinen, "Median robust extended local binary pattern for texture classification," *IEEE Trans. Image Process.*, vol. 25, no. 3, pp. 1368–1381, Mar. 2016.

[58] M. Alkhatib and A. Hafiane, "Robust adaptive median binary pattern for noisy texture classification and retrieval," *IEEE Trans. Image Process.*, vol. 28, no. 11, pp. 5407–5418, Nov. 2019.

[59] T. Song, J. Feng, L. Luo, C. Gao, and H. Li, "Robust texture description using local grouped order pattern and non-local binary pattern," *IEEE Trans. Circuits Syst. Video Technol.*, vol. 31, no. 1, pp. 189–202, Jan. 2021.

**ABDUL WAHAB MUZAFFAR** (Member, IEEE) received the Ph.D. degree in software engineering from the National University of Sciences and Technology (NUST), Islamabad, Pakistan, in 2017. He is currently an Assistant Professor with Saudi Electronic University, Saudi Arabia. He has participated in and presented his research at conferences in United Arab Emirates, Thailand, and the USA. His current research interests include model-driven software engineering, data and text mining, bioinformatics, and machine learning. He is also a reviewer of various scientific journals.

**FARHAN RIAZ** received the B.E. degree from the National University of Sciences and Technology (NUST), Islamabad, Pakistan, the M.S. degree from the Technical University of Munich, Germany, and the Ph.D. degree from the University of Porto, Portugal. Currently, he is serving as a Senior Lecturer with the School of Computer Science, University of Lincoln, U.K. His current research interests include biomedical signal and image processing, applied machine learning, and computer vision.

**TARIK ABUAIN** received the Ph.D. degree in artificial intelligence from the Center of Artificial Intelligence Technology, Department of Computer Science, National University of Malaysia (UKM), in 2016. He has been a full-time Assistant Professor with the Computer Science Department, Saudi Electronic University, Riyadh, Saudi Arabia, since 2016. His current research interests include artificial intelligence, machine learning, optimization, computer vision, deep learning, and the IoT.

**WALEED ABDEL KARIM ABU-AIN** received the Ph.D. degree in artificial intelligence from the Artificial Intelligence Technology Center, Department of Computer Science, National University of Malaysia (UKM), in 2016. Since 2016, he has been a full-time Assistant Professor with the Department of Computer Science, Applied College, Taibah University, Saudi Arabia. His current research interests include artificial intelligence, machine learning and optimization, data science, computer vision, deep learning, and the Internet of Things.

**FARHAN HUSSAIN** received the master's and Ph.D. degrees in electronics and computer engineering from Hanyang University, Seoul, South Korea. He is currently an Associate Professor with the Department of Computer and Software Engineering, College of Electrical and Mechanical Engineering, National University of Sciences and Technology. He has published various research papers in various international journals and conferences. His current research interests include convolutional neural networks, deep learning, machine learning, image and video processing/compression, NAND-based flash memories, and memory systems.

**MUHAMMAD UMAR FAROOQ** received the master's degree in computer science from Quaid-i-Azam University, Pakistan, the master's degree in software engineering from the National University of Sciences and Technology, Pakistan, and the Ph.D. degree in computer science from the University Politehnica of Bucharest, Romania. He is currently an Assistant Professor of computer and software engineering with the College of Electrical and Mechanical Engineering, National University of Sciences and Technology. He is an inventor of one awarded U.S. patent, a reviewer of several international conferences and journals, and the author of several international publications. His research interests include routing and MAC protocols for wireless ad hoc networks, delay-tolerant networks, and the Internet of Things.

**MUHAMMAD AJMAL AZAD** received the Ph.D. degree in electrical and computer engineering from the University of Porto, Portugal. He is currently a Senior Lecturer of cyber security with the Department of Computer Science and Digital Technologies, Birmingham City University. His current research interests include network security, privacy, and machine learning.